

## Research Article

# Influence of Surfactant on the Morphology and Photocatalytic Activity of Anatase TiO<sub>2</sub> by Solvothermal Synthesis

Junfang Wei <sup>1,2</sup>, Xiaojing Wen,<sup>1,2</sup> and Fang Zhu <sup>3</sup>

<sup>1</sup>School of Resources and Materials, Northeastern University at Qinhuangdao, Northeastern University, Qinhuangdao, China

<sup>2</sup>Key Laboratory of Dielectric and Electrolyte Functional Material Hebei Province, School of Resource and Materials, Northeastern University at Qinhuangdao, Qinhuangdao, China

<sup>3</sup>School of Computer and Communication Engineering, Northeastern University at Qinhuangdao, Northeastern University, Qinhuangdao, China

Correspondence should be addressed to Junfang Wei; [weijunfang@neuq.edu.cn](mailto:weijunfang@neuq.edu.cn)

Received 6 February 2018; Revised 7 May 2018; Accepted 10 June 2018; Published 5 July 2018

Academic Editor: Giuseppe Compagnini

Copyright © 2018 Junfang Wei et al. This is an open access article distributed under the Creative Commons Attribution License, which permits unrestricted use, distribution, and reproduction in any medium, provided the original work is properly cited.

Highly photocatalytically active anatase TiO<sub>2</sub> were synthesized by a solvothermal method using tetrabutyl titanate (TBT), citric acid, and ethanol as raw material. The morphology and photocatalytic activity of titanium oxide have changed significantly with the presence of surfactants, such as cetyltrimethylammonium bromide (CTAB), sodium dodecylbenzenesulfonate (SDBS), and diethanolamine (DEA). Scanning electron microscope and X-ray powder diffraction results show that the synthesized products are anatase TiO<sub>2</sub> spherical particles with a micronanostructure. The crystal type of TiO<sub>2</sub> has no obvious change with the addition of different surfactants, but the morphology, size, and dispersion of the TiO<sub>2</sub> particles have changed to some extent. Among the three surfactants, CTAB is beneficial to reduce TiO<sub>2</sub> particle size and improve TiO<sub>2</sub> dispersion and agglomeration. DEA is favor to self-assembly the nanocrystals into spherical particles. Degradation of methyl orange photocatalyzed by TiO<sub>2</sub> prepared with CTAB as surfactant reaches 95.4% under ultraviolet light for 100 min. After five recycles, the catalyst did not exhibit significant loss of photocatalytic activity, confirming that the photocatalyst is essentially stable. This work indicates that the surfactant-assisted solvothermal method is an effective approach to improve the structure, morphology, and photocatalytic performance of TiO<sub>2</sub>. Moreover, the surfactants with various types can interact with the precursors of TiO<sub>2</sub> in different ways.

## 1. Introduction

Among various types of photocatalysts, titanium dioxide (TiO<sub>2</sub>-) assisted photocatalytic oxidation has received much attention in the last few years due to its nontoxicity, strong oxidizing power, and long-term photostability [1–7]. These remarkable advantages originate from the unique physical and chemical properties of TiO<sub>2</sub> which depend not only on the crystal phase and particle size but also on the particle morphology. Therefore, controlling the morphology of TiO<sub>2</sub> nanoparticles is of key importance in the fabrication of materials with desired photocatalytic properties [8–12]. Over the past decades, a variety of controlled synthesis methods have been attempted to synthesize well-defined particles with varied morphologies [13, 14]. Compare with the sol-gel method, the solvothermal method not only

enables obtaining materials with a large surface area and high crystallinity but also flexibly adjust the parameters to control the morphology of products. In the course of solvothermal synthesis, the reaction path is very sensitive to the experimental conditions. Also, it is of practical importance to select suitable surfactant molecules, which act as templates or shape controllers, directing the formation of a structure toward a desired target arrangement [15]. The modification of TiO<sub>2</sub> nanoparticles with surfactant is an effective method to control their morphologies and structures. Wang et al. [16] reported a simple synthetic approach based on the solvothermal technique with oleic acid (OA) and oleylamine (OM) as two surfactants for preparation of TiO<sub>2</sub> nanocrystals with different morphologies such as elongated rhombic, dog-bone, oval, and core-shell structure. Leng et al. [17] demonstrated a surfactant-assisted exfoliation method to synthesize TiO<sub>2</sub> 2D

nanosheets and revealed that tetrabutylammonium hydroxide as a cationic surfactant played a crucial role in retaining the 2D nanosheet structures. Lekphet et al. [18] studied the effect of amounts of tetramethylammonium hydroxide (TMAH) surfactant on the morphology and size of TiO<sub>2</sub> particles. Obviously, TiO<sub>2</sub> assisted by different kinds of surfactants show various morphologies. However, few complete comparison has been made in the past years about the interactions between different kinds of surfactants and the precursors of TiO<sub>2</sub>.

In this paper, we reported a simple solvothermal method by using surfactants to make well-defined highly crystalline mesoporous anatase TiO<sub>2</sub>. Herein, CTAB, SDBS, and DEA as the typical anionic, cationic, and nonionic surfactants were introduced into the solvothermal system to prepare the TiO<sub>2</sub> nanoparticles with diverse morphologies, respectively. The structural and morphologic changes of TiO<sub>2</sub> nanoparticles were compared. The as-prepared TiO<sub>2</sub> nanoparticles were used in the comparative study in the photocatalytic degradation of methylene orange (MO) solution under UV light irradiation. TiO<sub>2</sub> were prepared here by a surfactant-assisted solvothermal approach to provide a valuable and interesting way for further improving the photocatalytic activities and stability.

## 2. Experimental Sections

**2.1. Materials.** All of the chemical reagents were of analytical purity and used without further purification.

**2.2. Catalyst Preparation.** TiO<sub>2</sub> was prepared via a facile one-step solvothermal process. Briefly, 30 mL TBT's ethanol solution (1.3 mol/L) was added drop by drop to 20 mL ethanol solution containing quantitative citric acid and surfactant (10 mmol) under stirring. After vigorously stirring for 60 min at room temperature, the as-formed mixture was transferred to a 100 mL Teflon-lined stainless steel autoclave, sealed, and then heated at 180°C for 24 h. After cooling to room temperature, the white precipitates were collected by a centrifugation and washed with ethanol and distilled water for three times, respectively. The samples were dried overnight at 80°C. Then, the dried masses were calcined at 460°C for 30 min in air atmosphere to remove the organics adsorbed on the surface. The as-prepared samples are referred to a (without surfactant), b (with CTAB as surfactant), c (with SDBS as surfactant), and d (with DEA as surfactant), respectively.

**2.3. Characterization.** The samples were studied by X-ray diffraction (XRD, DX-2500) using Cu K $\alpha$  radiation ( $\lambda = 1.5406 \text{ \AA}$ ) from  $2\theta = 20\text{--}80^\circ$  at a scan speed of  $0.08^\circ/\text{s}$ . The microstructure of the particles was characterized by a scanning electron microscope (SEM, ZEISS SUPRA55). FT-IR studies were performed on a Shimadzu-8400S spectrometer for confirmation of the surfactant presence and surface hydroxyl functional group. The special-surface area and pore size distribution were estimated by the Brunauer-Emmett-Teller (BET.SSA-4300) multiple points' method, based on the nitrogen gas adsorption isotherm (77 K).

**2.4. Photocatalytic Reduction Test.** The prepared samples were subjected to liquid phase photocatalytic evaluation using a self-made photocatalytic reactor. The photocatalytic experiments were examined by adding 200 mg TiO<sub>2</sub> powder into a quartz tubes (120 mL) containing 50 mL of the MO aqueous solution (25 mg/L). The suspension was kept stirring (500 r/min) in the dark for 1 h to reach the adsorption-desorption equilibrium prior to the irradiation, and the initial absorbance of the MO aqueous solution was recorded as  $A_0$ . After that, a 250 W mercury lamp was opened as an ultraviolet-visible light source. The power density of the lamp on the solution (20 cm away from the photocatalytic reactor) is  $43.5 \text{ mW/cm}^2$ . During the UV light irradiation, 2 mL of the suspension solution was extracted at every 20 min intervals and the solution was separated from the catalyst through centrifugation. The value of MO concentration was checked on the basis of its UV-vis absorption which measured by the UV-vis spectrophotometer (772S Jingke Shanghai) at 461 nm.

The photodegradation percentage was estimated as follows:

$$\omega = \left( \frac{A_0 - A_t}{A_0} \right) \times 100\%, \quad (1)$$

where  $A_0$  is the initial absorbance of MO aqueous solution after the adsorption-desorption equilibrium and  $A_t$  is the absorbance of methyl orange at reaction time  $t$  (min).

After washing with ethanol and deionized water for several times, the recycled catalyst (sample b) was redispersed in 50 mL of MO solution and the new photocatalytic cycle began. The photocatalytic activity of recycled catalyst was also measured under the same conditions as reference.

## 3. Results and Discussion

**3.1. Characterization of Photocatalyst.** The SEM images in Figure 1 confirm the effect of surfactants on the morphology and particle size of TiO<sub>2</sub>. SEM images reveal that the irregular spherical nanobundles (Figure 1(d)), relatively uniform nanospheres (Figure 1(b)), and not uniform spherical nanoparticles (Figure 1(c)) are prepared by applying DEA, CTAB, and SDBS as surfactants, respectively (Figures 1(b)–1(d)). It seems that when the surfactant type changes, the grain size and aggregation of TiO<sub>2</sub> are different. It is generally considered static repulsion and special hindrance from the reaction of interfacial energy among particles that could prevent the aggregation of nanometer particles [19]. In general, the formation of TiO<sub>2</sub> in the solvothermal system mainly depends on the hydrolysis rate of TBT and the growth rate of nuclei. In acidic solution, a large number of hydrolytic micelles form rapidly due to the hydrolysis of TBT. The adsorption of H<sup>+</sup> makes the micelles with positive charges and produces the electrostatic repulsion by the polar groups of the CTBA barrier and steric hindrance. On the other hand, CTAB has a large molecular size as a commonly used cationic surfactant. The cationic ion can attach to the negatively charged Ti-O<sup>-</sup> bonds, thus reduce their surface energy effectively, making the nanoparticles stable in solution. Based on the above

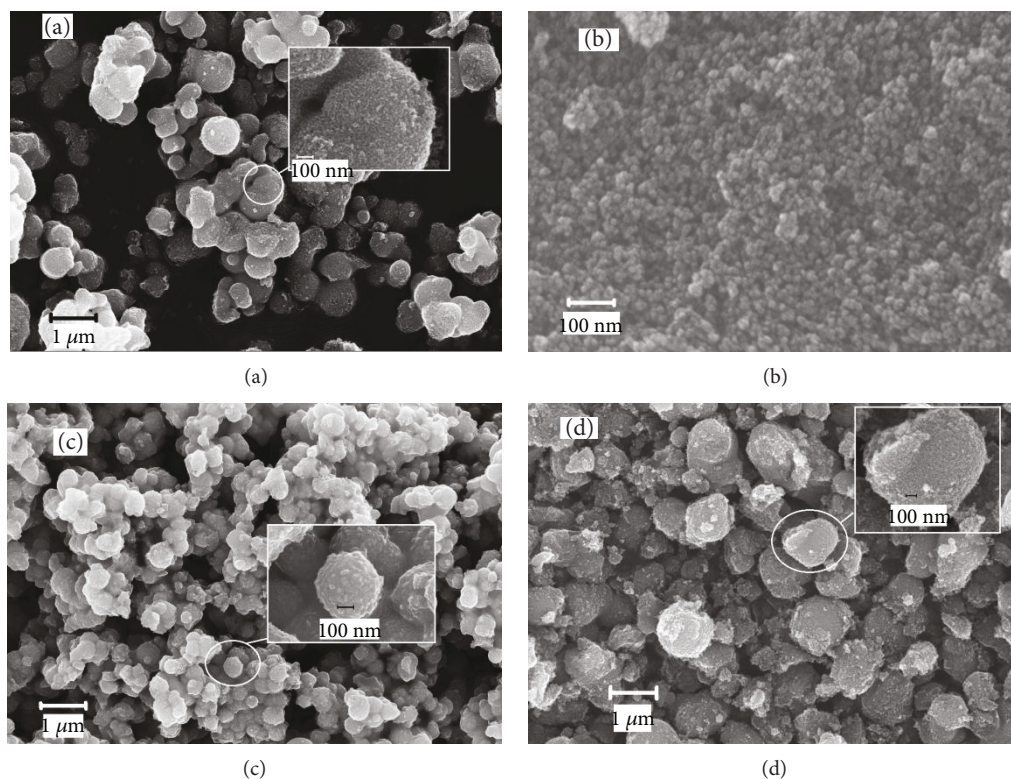


FIGURE 1: SEM images of  $\text{TiO}_2$  samples synthesized by different surfactants.

reasons, CTAB is the optimum surfactant for uniform spherical  $\text{TiO}_2$  nanoparticle preparation with small particle size in our solvothermal reaction conditions. In contrast to this, the anion SDBS induces the micelles to assemble, and thus not uniform spherical nanoparticles were synthesized. In addition, from the results of particle size distribution and morphology control, the effect of adding the nonionic surfactant DEA apparently is smaller than others. We speculate that static repulsion may have a significant impact on the shape and grain size control of  $\text{TiO}_2$  particles.

To characterize the crystal structure and crystallinity of  $\text{TiO}_2$  samples, XRD patterns were taken and illustrated in Figure 2. As observed in the XRD patterns of  $\text{TiO}_2$  samples, all nanostructured diffraction peaks are well matched to pure anatase  $\text{TiO}_2$  (JCPDS 89-4921). The peaks at  $2\theta = 25.3^\circ, 37.8^\circ, 48.0^\circ, 53.9^\circ, 55.0^\circ,$  and  $62.7^\circ$  were ascribed to the (101), (004), (200), (105), (211), and (204) crystallographic plane diffraction of anatase  $\text{TiO}_2$ , respectively, confirming that the presence of surfactants in the solvothermal system has no effect on the crystal structure of  $\text{TiO}_2$ . The intensity and width of XRD diffraction peak changed with the addition of surfactant, which indicated that the modification of surfactant had a certain effect on the grain growth. The average crystallite size of the samples calculated by applying the Scherrer equation and the relative crystallinity based on sample a were listed in Table 1. XRD results show that the crystallite size trend is consistent with the SEM results. With the addition of CTAB, the small particle size and favorable dispersion of  $\text{TiO}_2$  are achieved. Under the same synthesis conditions, the presence of surfactants can improve the crystallinity.

$\text{N}_2$  adsorption-desorption measurements indicate that the BET surface areas are  $b (83.45 \text{ m}^2/\text{g}) > d (76.31 \text{ m}^2/\text{g}) > c (67.64 \text{ m}^2/\text{g}) > a (49.09 \text{ m}^2/\text{g})$  (as in Table 1), respectively. Surfactants in the solvothermal system can inhibit  $\text{TiO}_2$  grain growth and increase particle dispersity. After thermal treatment, surfactants adsorbed in the  $\text{TiO}_2$  particles will decompose to produce  $\text{CO}_2$ , notably increasing the intrinsic pore volume and surface area. High surface area can provide more active sites, which is beneficial to the photocatalytic property. The pore size distribution of sample b calculated by the BJH model shows the presence of uniform nanopores with sizes of 3.2 nm which is typical mesoporous. The pore size distribution of sample b shows the presence of two sets of uniform nanopores with sizes of 2.2 and 13.0 nm (Figure 3(b)). These results indicate that the surfactant-assisted solvothermal system had a dramatic impact on the structure of as-prepared anatase  $\text{TiO}_2$  samples. High crystallinity and high porosity anatase  $\text{TiO}_2$  samples were obtained after thermal treatment in air at  $460^\circ\text{C}$  for 30 min. Specifically, during annealing in air, the adjacent nanocrystal building blocks can be cross-linked by removing surfactant molecules and the increasing oriented attractive forces can further lead to in situ three-dimensional crystallographic fusion to minimize the total system energy through reducing the high surface energy and eliminating the crystal defects, yielding mesoporous  $\text{TiO}_2$  spherical nanobundles [20].

The FT-IR spectra of as-obtained samples were exhibited in Figure 4. For the pure  $\text{TiO}_2$ , the absorption peaks at  $3400 \text{ cm}^{-1}$  and  $1630 \text{ cm}^{-1}$  are attributed to the hydroxyl group from water and Ti-OH, respectively, while the peak

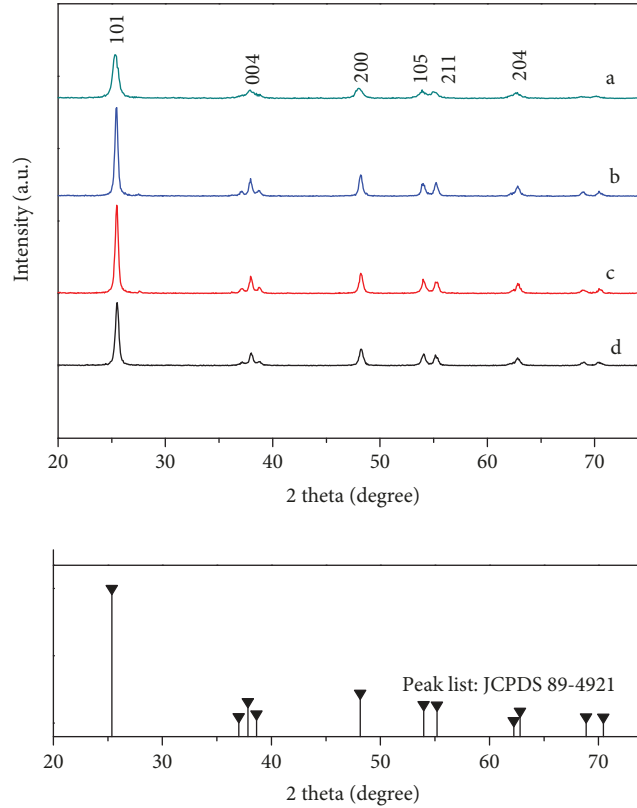


FIGURE 2: XRD patterns of  $\text{TiO}_2$  samples synthesized by different surfactants.

TABLE 1: The average crystallite size, relative crystallinity, and BET surface area of the samples.

| Samples | Relative crystallinity (%) | Average crystallite size (nm) | BET surface area ( $\text{m}^2/\text{g}$ ) |
|---------|----------------------------|-------------------------------|--|
| a       | 100                        | 24.5                          | 49.09                                      |
| b       | 125                        | 15.1                          | 83.45                                      |
| c       | 121                        | 28.2                          | 67.64                                      |
| d       | 103                        | 27.2                          | 76.31                                      |

situated at  $500\text{ cm}^{-1}$  could be assigned to the characteristic frequency of Ti-O-Ti. As for the samples a, b, c, and d, there are no significant differences of peak positions observed, indicating that the introduction of surfactants into the  $\text{TiO}_2$  synthetic system cannot alter the structure of  $\text{TiO}_2$ , which accords well with the XRD results. The area of absorption peaks at  $3400\text{ cm}^{-1}$  and  $1630\text{ cm}^{-1}$  increased significantly in sample b, which indicated that the introduction of CTAB can introduce more surface hydroxyl groups of the  $\text{TiO}_2$ . Photocatalytic chemical reactions occurring on the surface of semiconductor materials depend on the process, which starts from the absorption of light and results in attainment of photogenerated electrons and holes in the surface. The illuminated semiconductor surface is regarded as a producer of hydroxyl radicals (e.g.,  $\text{h}^+ + \text{OH}^- \rightarrow \cdot\text{OH}$ ). These and other highly oxidizing initial products of this indirect photochemical reaction go on to attack oxidizable contaminants.

Commonly, the enhancement of surface hydroxyl content on the surface of  $\text{TiO}_2$  is beneficial to the improvement of photocatalytic performance [21], which can be supported by the results of photocatalytic investigation.

Because  $\text{TiO}_2$  sample b have a large surface area ( $83.45\text{ m}^2/\text{g}$ ) and thus can offer abundant adsorption sites that are catalytically active, further investigations on the optical absorption property and electronic band structure of  $\text{TiO}_2$  sample b were performed. Figure 5 depicts the UV-vis diffuse reflectance spectrum of  $\text{TiO}_2$  sample b. The absorption peak appears at  $330\text{ nm}$  in Figure 5(a). The band gap may be calculated based on the absorption spectrum by utilizing Tauc's relationship [22]. The  $E_g$  of  $\text{TiO}_2$  sample b may be determined by extrapolating  $(\alpha h\nu)^2$  against  $h\nu$  at  $(\alpha h\nu)^2 = 0$  (Figure 5(b)). The energy gap quantity of the  $\text{TiO}_2$  sample b is calculated to be  $2.97\text{ eV}$  which is lower than that of typical anatase titanium oxide. Such differences in optical absorption properties and band edges of  $\text{TiO}_2$  sample b may be interpreted as numerous defects being generated upon fabricating the mesocrystalline architecture, which could then alter the electronic band structures of the products [23].

**3.2. Photocatalytic Activities of  $\text{TiO}_2$  Samples.** Photocatalytic activity tests were conducted by the self-sensitized degradation of MO in aqueous solution under ultraviolet light irradiation. Figure 6 shows the concentrations of MO with irradiation time for the four samples. It is clearly observed that all three samples synthesized by different surfactants

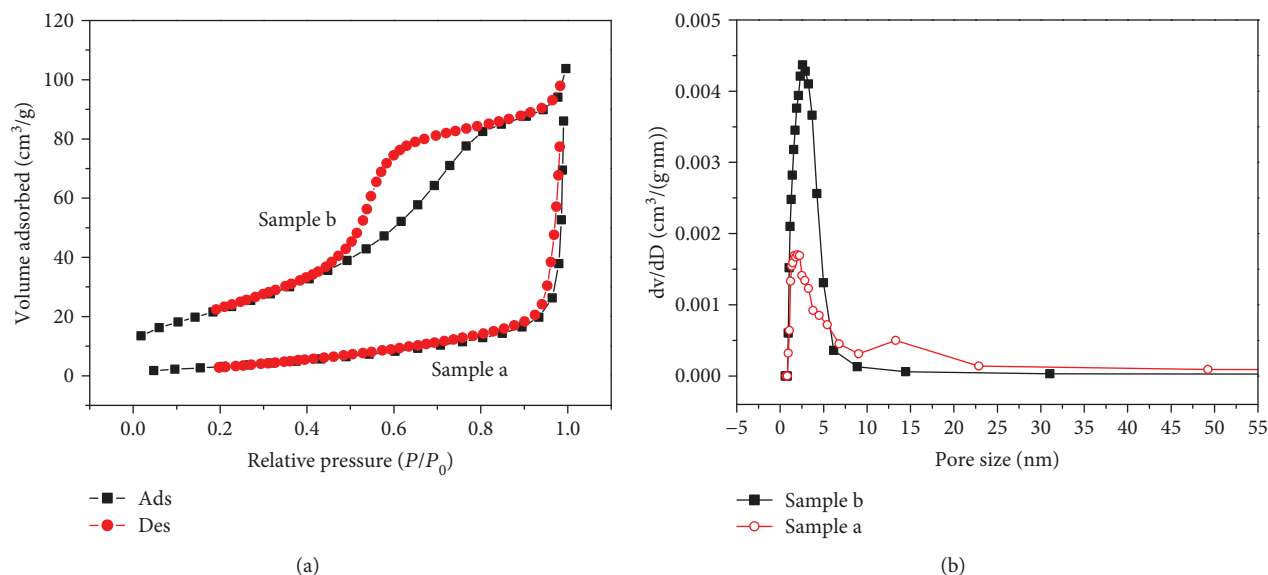


FIGURE 3:  $N_2$  adsorption-desorption isotherms (a) and pore size distribution (b) of samples a and b.

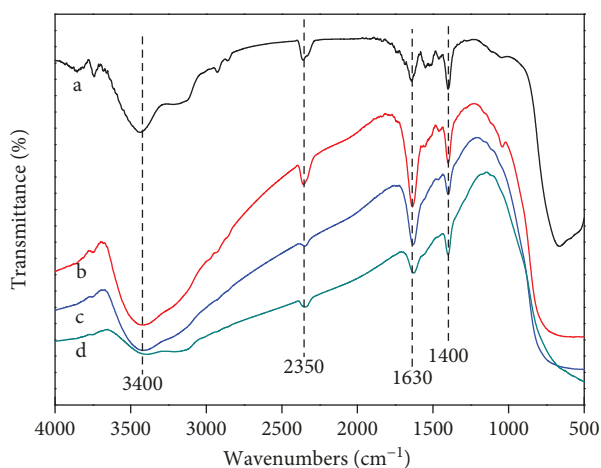


FIGURE 4: FT-IR spectra of  $TiO_2$  samples synthesized by different surfactants.

possess higher photocatalytic activity than the samples synthesized without surfactant. This indicates that the activities of the mesoporous  $TiO_2$  samples prepared by the solvothermal with surfactants are superior to the conventional sample in the dye self-sensitized degradation. Sample b is obviously the most active sample, and the order of photocatalytic activities is  $b > c > d > a$ .

It is well known that the photocatalytic activity of nanocatalyst is related to the grain size, specific surface area, adsorption capacity of the sample, and number of surface hydroxyl groups [24–26]. By introducing surfactants into the solvothermal system, the photocatalytic activity of  $TiO_2$  was improved in some extent. Among several kinds of surfactants, CTBA shows more significant modification. Due to electrostatic repulsion and steric hindrance of the CTBA barrier, the agglomeration and growth of  $TiO_2$  grain was inhibited,

the particle size of  $TiO_2$  was significantly reduced, and the specific surface area increased. The surfactants not only have great influence on the particle size and morphology of  $TiO_2$  but also affect the functional groups on the surface of  $TiO_2$ . The introduction of CTBA increases surface hydroxyl groups on the  $TiO_2$  surface, thereby the catalytic activity is improved.

Considering the stability of a catalyst is also important for its application; multiple runs for the degradation of MO upon sample b were performed. As shown in Figure 7, after five runs of photocatalytic reaction, the photocatalytic efficiency of sample b decreases only about 6.8% and the catalytic ability of sample b almost completely recovered after regenerating with distilled water, which may due to the adsorbed intermediates on the surface of the catalyst during the recycling experiments. The catalyst did not exhibit significant loss of activity. It indicates that the  $TiO_2$  particles synthesized by the solvothermal method with CTAB as surfactant have high stability, which is especially important for its application.

## 4. Conclusions

In summary, the high crystallinity anatase  $TiO_2$  with different morphologies was prepared by the solvothermal method using TBT as the titanium source and the surfactant in the ethanol system. Shape, size, and surface hydroxyl groups of  $TiO_2$  can be manipulated by using different surfactant compositions and concentrations during preparation. The  $TiO_2$  samples with different shapes and sizes show different photocatalytic activities. The novelty of this research is that through comparison, it was found that the static repulsion cationic surfactants played an important role on shape and grain size control. The introduction of CTAB in the solvothermal system could reduce the particle size and agglomeration of  $TiO_2$  particles and increase the specific surface area and surface hydroxyl groups of  $TiO_2$ , which could significantly

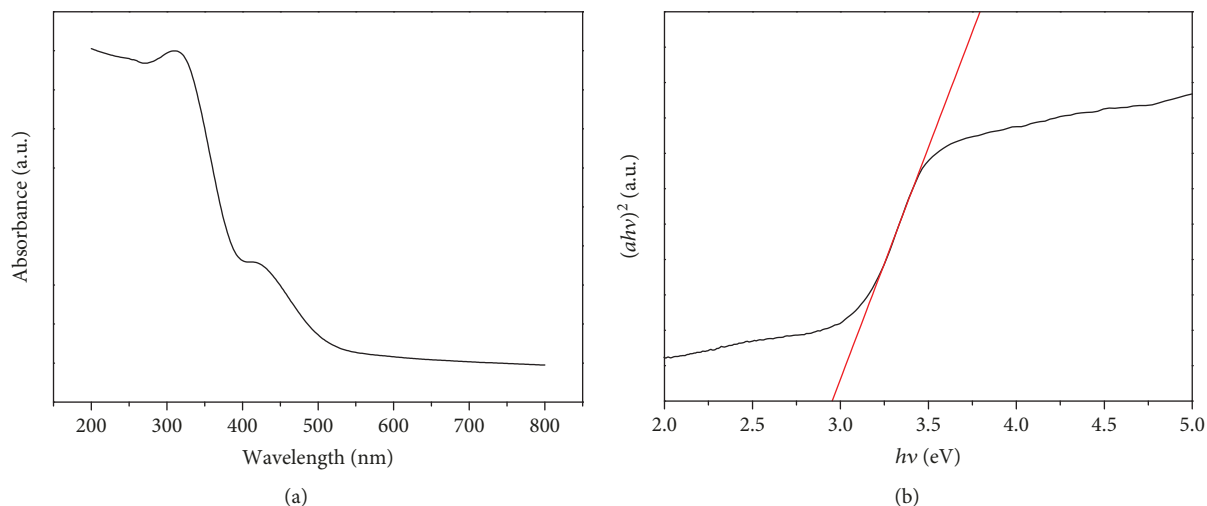


FIGURE 5: UV-vis diffuse reflectance spectrum (a) and plot to determine the band gap (b) of the TiO<sub>2</sub> sample b.

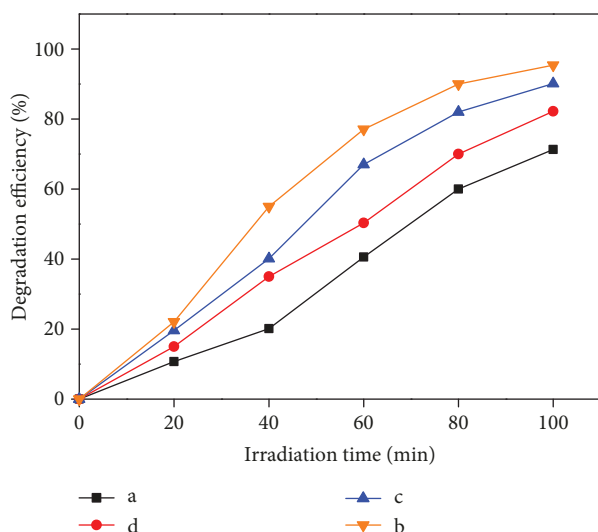


FIGURE 6: Degradation efficiency of TiO<sub>2</sub> samples synthesized by different surfactants.

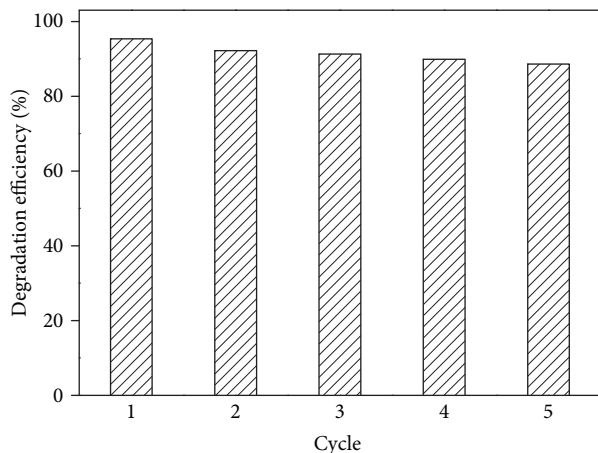


FIGURE 7: Recovery test of sample b.

improve the photocatalytic activity of TiO<sub>2</sub>. The degradation of methyl orange was 95.4% over the reference TiO<sub>2</sub> within 100 min. The degradation was not less than 90% of initial activity after 5 times of recycling. In the solvothermal synthesis of TiO<sub>2</sub> and other oxide photocatalysts, these findings will be greatly useful in controlling the microscopic and macroscopic morphologies of the nanomaterials.

### Data Availability

The data used to support the findings of this study are available from the corresponding author upon request.

### Conflicts of Interest

The authors declare that they have no conflicts of interest.

### Acknowledgments

This project was supported financially by the Fundamental Research Funds for the Central Universities (no. N162304012).

### References

- [1] A. Ajmal, I. Majeed, R. N. Malik, H. Idriss, and M. A. Nadeem, "Principles and mechanisms of photocatalytic dye degradation on TiO<sub>2</sub> based photocatalysts: a comparative overview," *RSC Advances*, vol. 4, no. 70, pp. 37003–37026, 2014.
- [2] T. Jafari, E. Moharreri, A. Amin, R. Miao, W. Song, and S. Suib, "Photocatalytic water splitting—the untamed dream: a review of recent advances," *Molecules*, vol. 21, no. 7, p. 900, 2016.
- [3] M. Ge, C. Cao, J. Huang et al., "A review of one-dimensional TiO<sub>2</sub> nanostructured materials for environmental and energy applications," *Journal of Materials Chemistry A*, vol. 4, no. 18, pp. 6772–6801, 2016.
- [4] M.-Z. Ge, C.-Y. Cao, J.-Y. Huang et al., "Synthesis, modification, and photo/photoelectrocatalytic degradation applications

- of TiO<sub>2</sub> nanotube arrays: a review,” *Nanotechnology Reviews*, vol. 5, no. 1, pp. 75–112, 2016.
- [5] Y. Zhang, Z. Jiang, J. Huang et al., “Titanate and titania nanostructured materials for environmental and energy applications: a review,” *RSC Advances*, vol. 5, no. 97, pp. 79479–79510, 2015.
- [6] Y. P. Que, J. Weng, L. H. Hu, J. H. Wu, and S. Y. Dai, “High open voltage and superior light-harvesting dye-sensitized solar cells fabricated by flower-like hierarchical TiO<sub>2</sub> composed with highly crystalline nanosheets,” *Journal of Power Sources*, vol. 307, pp. 138–145, 2016.
- [7] J. Bai and B. Zhou, “Titanium dioxide nanomaterials for sensor applications,” *Chemical Reviews*, vol. 114, no. 19, pp. 10131–10176, 2014.
- [8] H. Shibata, T. Ogura, T. Mukai, T. Ohkubo, H. Sakai, and M. Abe, “Direct synthesis of mesoporous titania particles having a crystalline wall,” *Journal of the American Chemical Society*, vol. 127, no. 47, pp. 16396–16397, 2005.
- [9] K. Zimny, T. Roques-Carnes, C. Carteret, M. J. Stébé, and J. L. Blin, “Synthesis and photoactivity of ordered mesoporous titania with a semicrystalline framework,” *Journal of Physical Chemistry C*, vol. 116, no. 11, pp. 6585–6594, 2012.
- [10] W. S. Chae, S. W. Lee, and Y. R. Kim, “Templating route to mesoporous nanocrystalline titania nanofibers,” *Chemistry of Materials*, vol. 17, no. 12, pp. 3072–3074, 2005.
- [11] C. Guo, M. Ge, L. Liu, G. Gao, Y. Feng, and Y. Wang, “Directed synthesis of mesoporous TiO<sub>2</sub> microspheres: catalysts and their photocatalysis for bisphenol A degradation,” *Environmental Science & Technology*, vol. 44, no. 1, pp. 419–425, 2010.
- [12] Z. Zheng, B. Huang, J. Lu, X. Qin, X. Zhang, and Y. Dai, “Hierarchical TiO<sub>2</sub> microspheres: synergetic effect of {001} and {101} facets for enhanced photocatalytic activity,” *Chemistry*, vol. 17, no. 52, pp. 15032–15038, 2011.
- [13] H. Park, Y. Park, W. Kim, and W. Choi, “Surface modification of TiO<sub>2</sub> photocatalyst for environmental applications,” *Journal of Photochemistry and Photobiology C: Photochemistry Reviews*, vol. 15, pp. 1–20, 2013.
- [14] S. Zinatloo-Ajabshir, S. Mortazavi-Derazkola, and M. Salavati-Niasari, “Schiff-base hydrothermal synthesis and characterization of Nd<sub>2</sub>O<sub>3</sub> nanostructures for effective photocatalytic degradation of eriochrome black T dye as water contaminant,” *Journal of Materials Science: Materials in Electronics*, vol. 28, no. 23, pp. 17849–17859, 2017.
- [15] J. H. Adair and E. Suvaci, “Morphological control of particles,” *Current Opinion in Colloid & Interface Science*, vol. 5, no. 1-2, pp. 160–167, 2000.
- [16] D. Wang, J. Yang, X. Li et al., “Preparation of morphology-controlled TiO<sub>2</sub> nanocrystals for the excellent photocatalytic activity under simulated solar irradiation,” *Materials Research Bulletin*, vol. 94, pp. 38–44, 2017.
- [17] M. Leng, Y. Chen, and J. Xue, “Synthesis of TiO<sub>2</sub> nanosheets via an exfoliation route assisted by a surfactant,” *Nanoscale*, vol. 6, no. 15, pp. 8531–8534, 2014.
- [18] W. Lekphet, T. C. Ke, C. Su et al., “Morphology control studies of TiO<sub>2</sub> microstructures via surfactant-assisted hydrothermal process for dye-sensitized solar cell applications,” *Applied Surface Science*, vol. 382, pp. 15–26, 2016.
- [19] F. Beshkar, S. Zinatloo-Ajabshir, S. Bagheri, and M. Salavati-Niasari, “Novel preparation of highly photocatalytically active copper chromite nanostructured material via a simple hydrothermal route,” *PLoS One*, vol. 12, no. 6, article e0158549, 2017.
- [20] Y. Liu, Y. Luo, A. A. Elzatahry et al., “Mesoporous TiO<sub>2</sub> mesocrystals: remarkable defects-induced crystallite-interface reactivity and their in situ conversion to single crystals,” *ACS Central Science*, vol. 1, no. 7, pp. 400–408, 2015.
- [21] J. B. Zhong, J. Z. Li, F. M. Feng et al., “Improved photocatalytic performance of SiO<sub>2</sub>-TiO<sub>2</sub> prepared with the assistance of SDBS,” *Journal of Molecular Catalysis A: Chemical*, vol. 357, pp. 101–105, 2012.
- [22] S. Moshtaghi, S. Zinatloo-Ajabshir, and M. Salavati-Niasari, “Nanocrystalline barium stannate: facile morphology-controlled preparation, characterization and investigation of optical and photocatalytic properties,” *Journal of Materials Science: Materials in Electronics*, vol. 27, no. 1, pp. 834–842, 2016.
- [23] U. Diebold, “The surface science of titanium dioxide,” *Surface Science Reports*, vol. 48, no. 5-8, pp. 53–229, 2003.
- [24] M. Ge, Q. Li, C. Cao et al., “Water splitting: one-dimensional TiO<sub>2</sub> nanotube photocatalysts for solar water splitting (Adv. Sci. 1/2017),” *Advanced Science*, vol. 4, no. 1, pp. 1–31, 2017.
- [25] M. Thomas, G. A. Naikoo, M. U. D. Sheikh, M. Bano, and F. Khan, “Effective photocatalytic degradation of Congo red dye using alginate/carboxymethyl cellulose/TiO<sub>2</sub> nanocomposite hydrogel under direct sunlight irradiation,” *Journal of Photochemistry and Photobiology A: Chemistry*, vol. 327, pp. 33–43, 2016.
- [26] M. Logar, I. Bračko, A. Potočnik, and B. Jančar, “Cu and CuO/titanate nanobelt based network assemblies for enhanced visible light photocatalysis,” *Langmuir*, vol. 30, no. 16, pp. 4852–4862, 2014.



**Hindawi**  
Submit your manuscripts at  
[www.hindawi.com](http://www.hindawi.com)

